Photonic Glasses: A Step Beyond White Paint

By *Pedro David García, Riccardo Sapienza,* and *Cefe López**

Self-assembly techniques are widely used to grow ordered structures such as, for example, opal-based photonic crystals. Here, we report on photonic glasses, new disordered materials obtained via a modified self-assembling technique. These random materials are solid thin films which exhibit rich novel light diffusion properties originating from the optical properties of their building blocks. This novel material inaugurated a wide range of nanophotonic materials with fascinating applications, such as resonant random lasers or Anderson localization.

1. Introduction

Extraordinary progress has been made in the fabrication of ordered nanophotonic structures displaying many novel optical properties. Material scientists have been enthusiastically involved in the field of ordered photonics, i.e., photonic crystals,[1,2] which has resulted, over the past twenty years, in continuous development of novel material techniques for accurate optical performance.[3] While (ordered) periodic photonic media take advantage of the periodicity in the dielectric constant and the consequent long-range correlation, disordered ones – with no positional order – can still strongly affect light transport.[4] Fractal media,[5] controlled disordered[6,7] and quasi-periodic[8] photonic crystals, and non-isotropic complex fluids, like nematic liquid crystals,[9] have the potentiality to combine the qualities of both random and periodic systems. Although artificially random media with novel properties, like polymer dispersed liquid crystals,[10] porous GaP[11] or Levy glasses,[12] have been proposed, a broad material-science effort into disordered photonics is still lacking. Although a number of interesting physical phenomena, such as coherent light backscattering,[13,14] random lasing,[15] strong light localization[16] and long-range intensity correlations,[17] have arisen from the study of such systems, these experiments have been mainly focused on materials like ''white paints'': oxides or semiconductor powders, such as TiO_2[18] or ZnO[19] in the visible region, and GaAs[20] or Ge[21] in the infrared. All such materials are formed by particles with casual shapes and sizes having a mean size on the order of the light wavelength. Materials composed of polydisperse spherical particles have also been used, presented both in solid arrangements, such as Al_2O_3,[22] ZnO[23] and TiO_2,[24,25] or in colloidal suspensions.[26,27] In all these cases, the particles composing the system are polydisperse in shape, size or both, and the individual electromagnetic response of each building block gives rise to an averaged-out optical response.[4] Up to now, disordered materials composed by monodisperse scatterers have not been available.

Here, we go a step beyond in the fabrication of disordered materials and introduce a new paradigm in the field of nano-photonics: the *photonic glass*. With the same building block – a dielectric sphere with size comparable to the wavelength of light – two extreme systems can be built: a perfectly ordered arrangement (a so-called *photonic crystal*) and a completely random arrangement of spheres (a so-called *photonic glass*). The most important property of both solid systems is the monodispersity of the building blocks that compose them, in this case polymer microspheres (with diameters from 200 nm to several microns and with a polydispersity of less than 2%). The disordered new compact and solid system is just an example of an old very well-known material[28] (in this case, polymer microspheres) arranged in a novel manner. It offers the possibility of probing a new range of interesting phenomena affected by the novel property of the monodispersity of the spheres. Figure 1a shows how the topological difference between a photonic glass and a photonic crystal leads to very different interference optical properties. A simple light transmission experiment can give a diffraction pattern for a photonic crystal (Fig. 1b) or a speckled pattern – a granular distribution of light intensity – for a photonic glass (Fig. 1c).

In this article we will show how photonic glasses have been demonstrated to be a perfect playground to observe dispersive light diffusion in the same system, a crucial combination which allows control of light diffusion as photonic crystals do for ballistic light. From the interplay between diffuse light and designed disordered materials, several effects may be observed including, for example, the possibility of self-tuned random lasers[15] or resonance-dependent Anderson localization.[16]

2. Photonic Glasses: Colloidal Instability

The key property necessary to achieve colloidal photonic crystals is colloidal solution stability. A colloid is a two-phase (at least) system in which one substance (the internal phase) is divided into

[*] Dr. P. D. García, Dr. Riccardo Sapienza, Prof. Cefe López
Instituto de Ciencia de Materiales de Madrid (CSIC) and Unidad Asociada CSIC-U. Vigo
C/Sor Juana Inés de la Cruz 3, 28049 Madrid (Spain)
E-mail: cefe@icmm.csic.es
Dr. P. D. García
DTU Fotonik, Department of Photonics Engineering
Technical University of Denmark
Ørsteds Plads 343, DK-2800 Kgs. Lyngby (Denmark)

DOI: 10.1002/adma.200900827

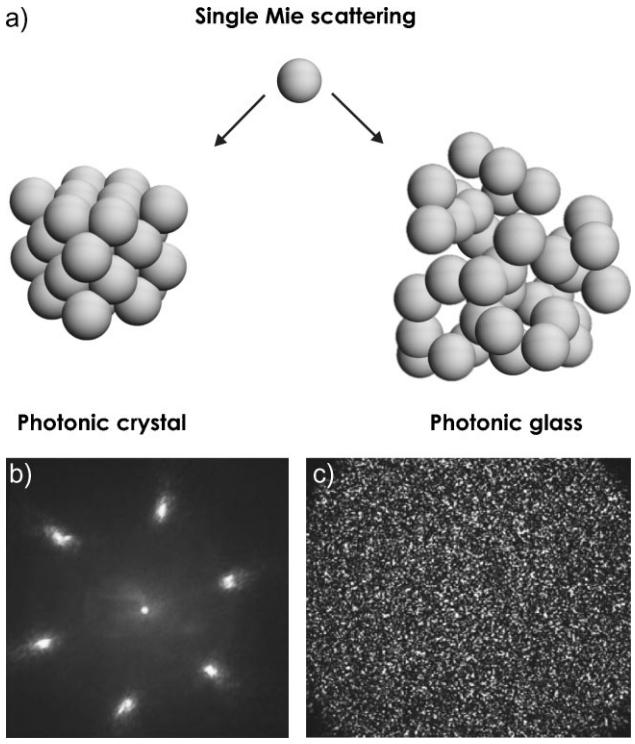

Figure 1. a) Ordered and disordered packing of a single-scattering particle, a dielectric sphere in this case. b,c) Light speckle pattern arising from an ordered face-centred cubic (fcc) arrangement of dielectric microspheres and from a random arrangement of the same spheres, respectively, and collected on a far-field screen.

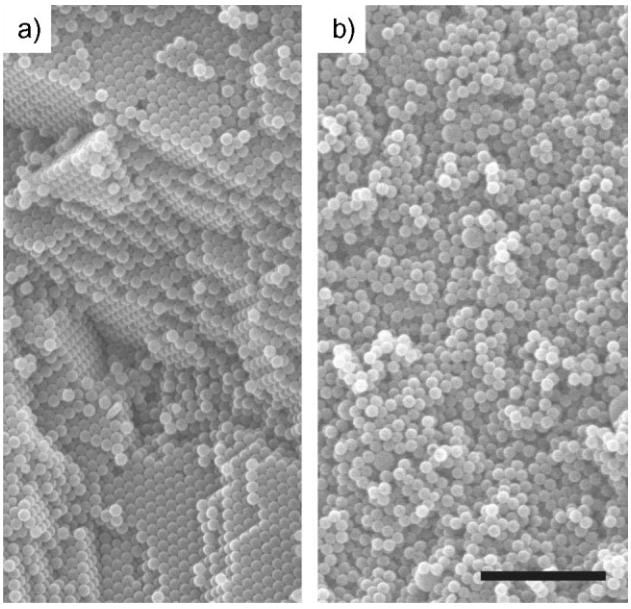

Figure 2. Incomplete disordered photonic crystal obtained by centrifugation. a) Top-surface SEM image, where spheres are ordered by the action of the water evaporation. b) Bottom-surface SEM image, where the spheres are arranged randomly by the effect of high-speed centrifugation. The scale bar is 15 μm

minute particles (colloidal particles), of between 1 nm and several microns, which are dispersed throughout a second substance (the external phase). The size is not the most important property of colloids, since the overwhelmingly important property of colloids is their very large surface area. To some degree, they are all surface and their properties are those of their surfaces. The large area emphasizes surface effects relative to volume effects, giving colloids properties different to those of bulk matter. Hereafter, we will only deal with sols composed of polymer spheres [poly(methyl methacrylate), PMMA, or polystyrene, PS] dispersed in a liquid (water).

Several methods have been tested to obtain disordered, solid and random arrangements of dielectric microspheres. The first, unsuccessful, attempts focused on mechanical perturbation of the colloidal suspension, for example, by forced sedimentation of microspheres by the action of high speed centrifugation. By placing a colloidal suspension of microspheres (either PS or PMMA) in a high-speed centrifuge (6 000 rpm), the sedimentation of the spheres is forced by the artificially increased gravity (∼1200 *g*, where *g* is the gravitational acceleration at the earth's surface). A solid white sediment is then obtained after evaporation of the solvent. Upon first examination, no colors are found in the reflectance from the bottom (system-substrate) surface of the sediment but, on the contrary, the top (system-air) surface shows visible iridescences due to Bragg reflections. A deeper inspection using scanning electron microscopy (SEM), shown in Figure 2, reveals a very high degree of ordering in the bulk material, corresponding to the top surface (Fig. 2a) and a random distribution of spheres corresponding to the bottom surface (Fig. 2b). This is an example of how ordered surfaces may hide very disordered bulk systems: a high reflectance from the surface of a sample it is not at all a proof of the existence of an underlying ordered structure. Reflectance measurements should be taken very carefully as characterization method. Transmittance measurements, on the contrary, may provide, in combination with reflectance ones, enough information from the bulk of the system.

A mechanical action over the colloidal suspension is not enough to force a random distribution of spheres; a second failed strategy followed this path. Opal-based photonic crystals (such as those shown in Fig. 2a) are usually grown by vertical deposition.[29] In this technique, a clean microscope slide is placed in a vial containing a colloidal suspension of spheres. By the action of water evaporation, the meniscus formed between the suspension and the substrate allows the spheres to self-assemble. The formation of the meniscus is, therefore, crucial and it is only possible if the substrate is hydrophilic. An initial hydrophobic microscope slide can be hydrophilized with a light chemical etching of it surface. Without this etching process, the formation of the meniscus is prevented on an otherwise hydrophobic substrate. This was tried in order to obtain a disordered arrangement of spheres – a photonic glass. Again, it failed and a very low quality photonic crystal was obtained, still showing Bragg iridescences from the surface. An important concept follows from this: bad photonic crystals are also bad photonic glasses.

The reason why these attempts failed is that the ordering of the spheres in an fcc structure takes place during water evaporation.

Some examples of not-completely-disordered systems can be found in the literature,[30] where traces of order reveal the invalidity of applying a mechanical method to obtain random arrangements of spheres. The water evaporation process and, in particular, surface tension are what force the spheres to self-assemble in an ordered fashion and it is this process that should be prevented. In order to do so, a more sophisticated method is needed. It is necessary to force the flocculation of the spheres and to induce the formation of random clusters to prevent the spheres from ordering. We pursued this strategy with the colloidal stability as the central argument. It is related to the surface charge of the particles, which ensures the suspension stability preventing them from sticking.[31,32] If two particles collide, they will stick together and make a bigger particle or, eventually, a cluster. Clusters get larger than the critical size to be suspended and settle.

In most lyophobic colloids, the particles are electrically charged with the same sign, and this keeps them apart, since they repel one another. Since lyophobic sols are stabilized by electric charge, adding extra charge (electrolytes) generally destroys the sol. For example, when rivers reach the sea with their loads of colloidal sediment, the ions in sea water coagulate the sol and the load is deposited, forming the delta.

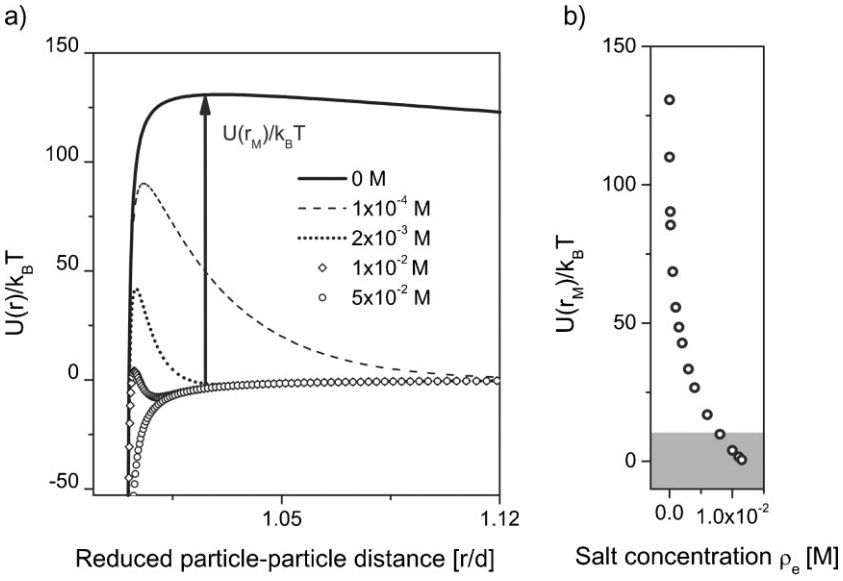

Figure 3. Left) Plot of the total interaction potential between two particles relative to the thermal energy as a function of the concentration of electrolytes in the suspension according to the proposed solution.[33] Right) The magnitude of $U(r_M)$, representing the potential barrier that prevents the colloids from flocculating. This barrier decreases when the electrolyte concentration increases. Energies bellow $10\,k_B\,T$ are shaded in grey. If the potential barrier is lower than this energy, the colloids flocculate. In this particular case, this happens for $\rho_e \geq 7.5 \times 10^{-3}$ M. The specific parameters used for this particular exemplification are a particle diameter $d = 1220$ nm with a surface potential $\psi = -30$ mV (measured with a standard electrophoretic mobility experiment) and the electrolytes (Ca^{2+} from $CaCl_2$) added to this suspension have $Z = 2$, with their concentration varying from $\rho_e = 0$ to 5×10^{-2} M.

The modeling of the sphere–sphere potential can be performed in the basis of Derjaguin-Landau-Verwey-Overbeek (DVLO) repulsion,[31,32] the detailed formulation of which can be found elsewhere.[33] Figure 3 plots the total interaction, $U(r)$, between two particles as a function of the electrolyte concentration. As a matter of fact, there is a high probability of flocculation as a result of the collision between two particles if the potential barrier $U(r_M) \leq 10\,k_B\,T$, where r_M is the reduced particle–particle distance at which $U(r)$ has the maximum value. This fact is pointed out in the right panel of Figure 3, where energies below these values are shaded in grey. For electrolyte concentrations for which $U(r_M) \leq 10\,k_B\,T$, the instability of the colloidal suspension is ensured and colloidal flocculation will occur. In this particular case, for an electrolyte concentration, $\rho_e = 1 \times 10^{-2}$ M, the potential barrier is $U(r_M) \sim 6\,k_B\,T$ and the Brownian energy is enough to force colloidal flocculation.

3. Preparation Method

The PS spheres employed to grow photonic glasses were synthesized by the Goodwin method,[34] which gives rise to a negative surface charge of the particles. PMMA spheres were synthesized following a similar method.[35] In both cases, positive electrolytes are needed to screen the negative surface charge of the colloids (which otherwise prevents natural agglomeration), which can be obtained by adding salts (which dissociate on dissolution, producing positive and negative ions) or acids (which again dissociate, producing protons and also negative radicals). The charge, Z, of the ions or the number of protons dissociated from an acid is an important parameter. The concentration of salt or acid needed to provoke the colloidal flocculation is inversely proportional to their charge. For example, half the concentration of a salt such as $CaCl_2$ (which dissociates to produce Ca^{2+} ions) is needed than of a salt such as NaCl (which dissociates producing Na^+ ions) to provoke colloidal flocculation. The attenuation of the repulsive potential gives rise to a net attractive potential between spheres. In this case, the number of effective collisions between spheres increases and clusters are formed by flocculation in the suspension. When the size of the clusters exceeds the critical size, they settle. The formation of clusters inhibits the self-assembling process that takes place during the liquid evaporation process and, consequently, a random distribution of disordered clusters is obtained.

In order to control the thickness and the area of the system, a methacrylate cylinder of height h and diameter d is glued with flexible and impermeable gum to a clean hydrophilic glass microscope slide (shown schematically in Fig. 4a). In a typical procedure, a total volume $V_T = 3$ mL of an aqueous suspension of PS spheres, 1220 nm in diameter, and $CaCl_2$ is prepared as follows: a volume $V_s = 2.5$ mL of a colloidal suspension of PS spheres with a concentration $\rho_s = 20$ g L^{-1} (2 wt.-%) is added to a volume $V_e = 60$ µl of $CaCl_2$ with a concentration $\rho^i_e = 0.5$ M. To reach the total volume, $V_w = 0.44$ mL of de-ionized water is added.

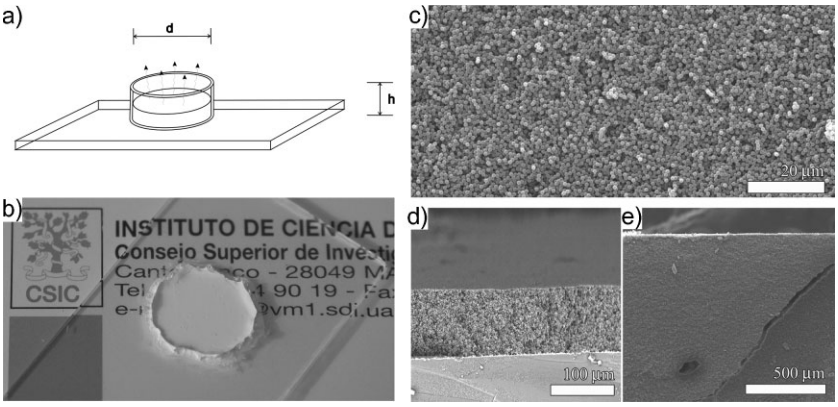

Figure 4. a) Schematic of the photonic glass growth method. A methacrylate cylinder with a height of $h \sim 1$ cm is fixed with impermeable gum to a clean, hydrophilic glass substrate. It is then filled with a charged colloidal suspension previously prepared and shaken under ultrasound. Then it is placed in an oven at constant temperature (~45 °C) to force the evaporation of the liquid phase. Finally, the methacrylate cylinder is removed from the glass substrate. b) Picture of a photonic glass grown on a substrate. The sample shows a high degree of planarity, apart from the irregularity of the edge. SEM images from different parts of a photonic glass made with PS spheres with $d = 1220$ nm: c) the surface of the sample, revealing the random arrangement of the spheres, and d,e) cleaved edges of the sample, revealing the planarity of the surface over a range of millimeters. The crack visible in image (e) is produced when removing the methacrylate cylinder from the glass substrate.

The final concentration of electrolytes in the final suspension is $[Ca^{2+}] = \rho_e^f = 0.01$ M. This aqueous suspension is shaken under ultrasound for 5 min to force the spheres to flocculate.

The cylinder, of diameter $d_c = 2$ cm, is then filled with the suspension and the solvent allowed to evaporate in an oven at constant temperature, typically at $T = 45$ °C. The sample is left inside the oven for a long enough to allow total evaporation of the liquid. When the liquid is completely evaporated, the cylinder is removed from the substrate, the photonic glass remaining attached to it (see a photograph and SEM images from the system in Fig. 4). In order to avoid possible cracking (Fig. 4c) or peeling of the sample from the substrate, it is important that the cylinder is not touching the substrate, leaving a small air chamber between the cylinder, the substrate and the gum.

As a matter of fact, a small fraction of colloidal suspension fills this air chamber by capillarity and the sample is more strongly attached to the substrate (see Fig. 4b). Proceeding this way, no cracking appears on removing the methacrylate cylinder from the substrate. The typical thickness obtained in this case is $t = (31 \pm 5)$ μm constant over a range of centimetres (see Fig. 4b and c). The thickness of the photonic glass is measured using a low magnification objective, taking measurements when focusing on the substrate and the glass surface, and subtracting. If the salt concentration is increased, the repulsive barrier is lowered and, consequently, the size of the clusters formed by flocculation is increased. If the salt concentration increases, the number of effective collisions required to attach two particles decreases. Figure 5a–d shows four SEM images corresponding to four different electrolyte concentrations in the colloidal suspension, respectively: $\rho_e = 0$, 2×10^{-3}, 1×10^{-2}, and 5×10^{-2} M. It is directly evident how the self-assembly process is inhibited by adding ions to the colloidal suspension. In the case of $\rho_e = 0$ M (Fig. 5a), the fcc arrangement of spheres is similar to that obtained by the vertical deposition method (Fig. 5a, inset). For this concentration, the electrostatic barrier is about 130 times the thermal energy; the spheres cannot flocculate but they do self-assemble during the evaporation process. In the case of $\rho_e = 2 \times 10^{-3}$ M (Fig. 5b), the electrostatic barrier is 20 times the thermal energy; the spheres are randomly distributed but the image still shows traces of short-range order (see Fig. 5b, inset). In this case, the repulsive barrier, $U(r_M) \sim 40\, k_B\, T$, is higher than the thermal energy of the particles, but the spheres coagulate and the system looks randomly arranged, apart from small ordered clusters. Even by incorporating recent modifications, the DLVO theory does not predict experimental results acceptably well which, generally, show that suspensions have lower stability than predicted.[36] For $\rho_e = 1 \times 10^{-2}$ M (Fig. 5c), the spheres are homogeneously and randomly distributed in the system; in this case, the electrolyte concentration is the optimal to provide a uniform distribution of spheres. Finally, in the case of $\rho_e = 5 \times 10^{-2}$ M (Fig. 5d), such a high electrolyte concentration gives rise to a totally attractive potential between colloids, which enhances the number of effective flocculating collisions and the formation of bigger clusters (see Fig. 5d, inset). The size of the clusters has an important effect on the filling fraction, f, of the system and may strongly affect the physical magnitudes that describe light transport. Thus, we showed that increasing the electrolyte concentration during the formation of glasses allows clusters of increasing size to be grown. Figure 5e plots the average f from different photonic glasses as a function of the electrolyte concentration from 0.74 (the expected theoretical volume for a perfect fcc structure[37]) to 0.55. These measurements have been performed by measuring the total mass and volume of the samples. The volume occupied by the PS spheres is estimated by weighing the substrate before and after sample growth. By doing so, we can estimate the sample weight. Furthermore, the total volume of the glass is obtained by measuring the thickness and sides of the samples with the microscope. Large error bars come from the total volume measurements. In particular, the measurement of the glass sides introduces a large error in the final value fo filling fraction, due to the irregularity of the sample edges (see Fig. 4b).

Photonic glasses are not only interesting as passive structures but also as host systems for light sources. With the aim of controlling emission properties by photonic structures, it is necessary to engineer a controlled way to include light emitters in the photonic matrices. Photonic glasses are good candidates to control diffuse emission properties, just as photonic crystals have been demonstrated to be optimum playgrounds to study light emission.[38] The availability of an active resonant system as the photonic glass is of paramount importance for tuning the diffuse emission properties of light emitters with the help of resonant collective response, as will be shown in the last section.

Active disordered materials have been usually obtained by simply grinding an active laser crystal[39] or just adding a gain

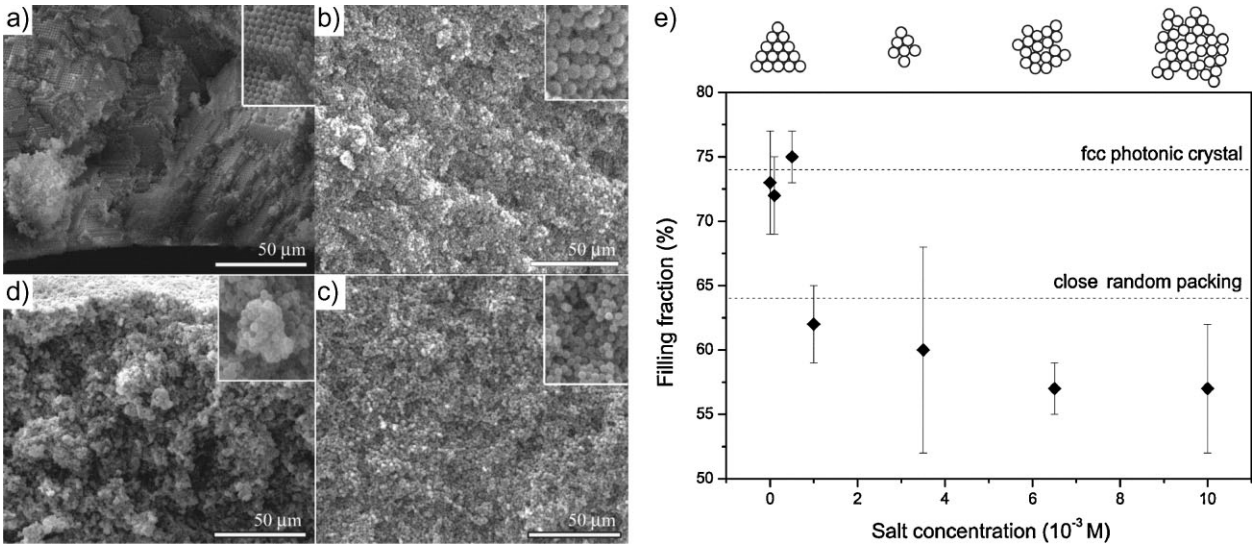

Figure 5. SEM images from colloidal suspensions of PS spheres with $d = 1220$ nm, naturally sedimented and after liquid phase evaporation. The colloidal suspensions were prepared with different electrolyte concentrations: a) $\rho_e = 0$ M, shows an ordered fcc arrangement of spheres (see crystallographic planes in the inset of the figure); b) $\rho_e = 2 \times 10^{-3}$ M, spheres are randomly distributed but still show ordered clusters (see inset); c) $\rho_e = 1 \times 10^{-2}$ M, the image shows a uniform random arrangement of spheres similar to the one in figure 2c.; and, d) $\rho_e = 5 \times 10^{-2}$ M, image shows a very inhomogeneous random distribution of spheres. e) Plot of the average f of a photonic glass as a function of electrolyte (salt) concentration. Spheres which composed the glass are 1220 nm diameter. The filling fraction can be estimated by weighting the samples when their geometry is known. A concentration 0 M gives rise to a well-known opal-based photonic crystal where the total volume occupied by the spheres is 74% of the total volume of the unit cell in an fcc lattice.

medium, quantum dots or organic dyes to white paints,[40] ceramics,[41] organic composites,[42] and even biological tissue.[43] In all those systems, the optical response is, again, monotonically dependent on the light wavelength over a wide range of energies. There is an interesting alternative way introduce an active medium in the photonic glass that, at the same time, can be used to destabilize the colloidal suspension. The gain medium, DCM (4-dicyanomethylene-2-methyl-6-dimethylaminostyryl-4H-pyran) dye, molecules are intercalated into the helices of the biopolymer deoxyribonucleic acid (DNA)[44a] to prevent the quenching of the dye and also to provide a way to dissipate the extra heat, due to optical pumping, in the DNA strands. In such a nano-designed gain medium, the intensity of the fluorescence is greatly enhanced. The DNA hosts charge ions in certain strand positions: it is a charged polymer. The whole emitter has, therefore, a net charge concentration of about 3×10^{-6} M. This extra amount of charge, when added to the colloidal suspension of PS microspheres, is enough to force the flocculation of the colloidal particles and, once the solvent is evaporated, a solid active photonic glass based on PS spheres coated by few nm of a DCM/DNA gel is obtained.[44b]

4. Optical Properties

The most remarkable property of photonic glasses is the resonant behavior in diffuse light when it is propagating through them. When light propagates in air or a glass slab, it travels from the source to the detector in a straight line. Light propagation through a homogenous medium is ballistic, that is, propagation direction is not changed during the process. If scattering particles are added to a homogenous film, the light propagation direction becomes more and more randomized. When light travels through a very disordered system, is multiply scattered and ballistic propagation can no longer accurately describe its transport. In multiple scattering dilute media, light transport can be accurately described as a diffusion process. In that case, interference effects can be obviated to a first approximation and light propagates like water poured over sand in a river delta. Processes described by diffusion are ubiquitous in nature: from molecules under a pressure gradient to (matter, electromagnetic, sound or seismic) waves in random systems. Light entering a disordered media is scattered (elastically) numerous times and, when it emerges from the material, the color of the incident light is till preserved, whatever the detected incident direction. Since ambient light covers the full visible spectrum, the diffusive medium appears white. All white materials used as white paint owe their color to multiple light scattering.

Photonic crystals instead exhibit color variations that are related neither to absorption bands, as in standard pigments, nor to Bragg scattering, as in photonic crystals. The optical properties of photonic glasses lie in the light-scattering response of the dielectric spheres of which it is composed. A single dielectric microsphere with size comparable to the wavelength of light (a Mie sphere), can sustain electromagnetic resonances.[45] When all the spheres are identical (within ~2% in our case), these modes occur all at the same frequency and, thus, are not washed out. In a macroscopic photonic glass, the diffuse-like transport of light is therefore strongly affected by the Mie modes. It is possible to observe resonances in the light transport. These electromagnetic modes are excited when the electromagnetic field wavelength is comparable with the optical diameter of the spheres. Those resonances have been probed by static and dynamic experiments as an extended optical characterization of photonic glasses. A

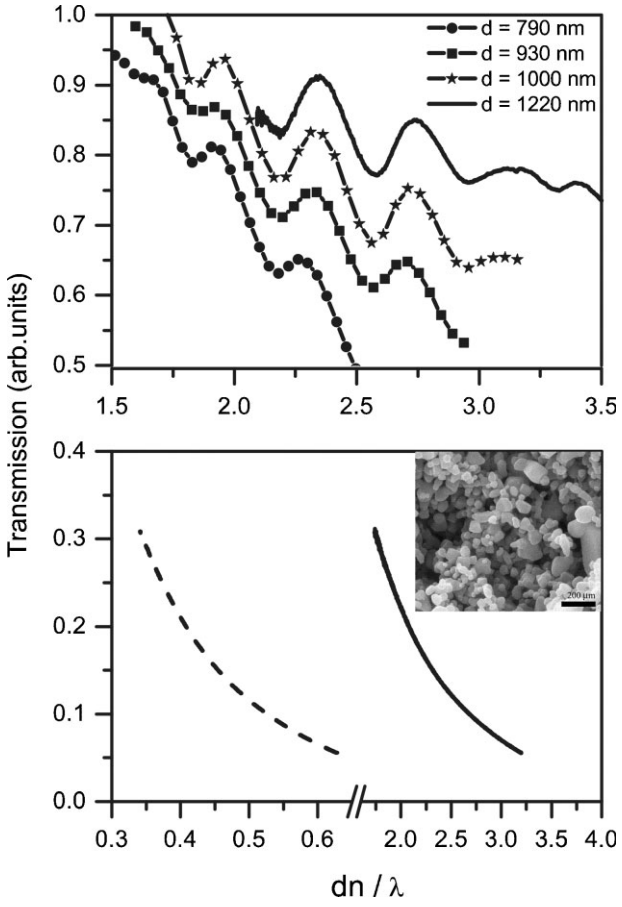

Figure 6. a) Normalized total transmission of white light through photonic glasses as a function of the reduced parameter $d \cdot n/\lambda$. Samples are composed of spheres with four different diameters and the thickness is about 100 μm in all cases. b) Total transmission of white light through two different reference samples as a function of the reduced parameter $d \cdot n/\lambda$. The dashed line represents total transmission through photonic glasses made of PS spheres of $d = 200$ nm. Solid-line represents total transmission through a powder made of polydisperse TiO_2 of averaged $d = 850$ nm (inset is an SEM image of the sample; the scale bar represents 200 nm). Both present non-resonant light transmission.

detailed optical study of the resonant behavior of diffuse light transport through such a system has also been recently provided.[46] By means of independent static and dynamic measurements, resonances have been shown in the transport mean free path, the diffusion constant and, also, the energy velocity of light.

Figure 6 shows direct measurements of the total diffuse light transmission through different photonic glass slabs (thickness $L \sim 100$ μm) upon white light illumination (500–920 nm). In order to be able to compare the optical response of different sphere sizes (790, 930, 1000, and 1220 nm), the measurements are plotted as a function of rescaled energy ($d \cdot n/\lambda$), where n is the refractive index. Oscillations in transmission and its spectral dependence are due to the existence of modes for the electromagnetic field in the spheres. The spectral positions of these Mie modes depend exclusively on the sphere diameter, d, and refractive index, n. Figure 6a shows clear and simple evidence of the resonant behavior of light transport in a broad energy interval. In order to remark on this fact, and also to clarify the conditions under which the modes can be collectively excited, the resonant behavior of these four different spheres sizes was compared with two different non-resonant dielectric random systems. Figure 6b plots the total transmission through two reference samples that, for different reasons, do not exhibit resonant behavior. As can be seen, there is no trace of resonance in the transport of light for these two reference systems. The first one (dashed curve) is a photonic glass composed of PS spheres with a diameter of 200 nm. The small size of the spheres compared to the light wavelength illumination, $(d \cdot n/\lambda) \sim 0.4$, means that their modes have energies in other ranges. Therefore, those spheres behave, upon this particular light energy illumination, as point-like scatterers, giving rise to Rayleigh scattering (where the structure of the scatterer can be neglected) instead of Mie scattering (where resonances can be sustained). Resonances are expected in other energy ranges (in the UV) for this particular system. The second reference (solid curve) is composed of TiO_2 non-spherical powders with a polydispersity of about 36% (Fig. 6b, inset) and a mean diameter of about 850 nm. A different situation arises with the non- resonant light transport through TiO_2 powder. In this case, the TiO_2 particles are large enough ($d \cdot n/\lambda \sim 2.5$) to sustain Mie modes in this wavelength interval. However, Figure 6b shows no trace of oscillations in the light transport because the resonances are smoothed out by polydispersity and the arbitrary non-spherical shape of the scatterers. Mie modes are defined by the morphology of the scatterer. When the scatterers are non-spherical and also polydisperse, as in the TiO_2 case, each building block sustains resonances for different wavelengths, which smoothes out the collective response and gives rise to an overall non-resonant behavior.

5. Self-Tuned Random Lasing

Fascinating phenomena can occur when optical gain is added to a photonic glass. For high enough optical gain, light fluorescence can be amplified by stimulated emission up to a level that lasing can occur. This is the so-called random lasing[15] and it is a special form of lasing that takes places in disordered materials with gain, where multiple scattering of light serves to obtain gain larger than losses and reach gain saturation, the fundamental mechanism that leads to coherence.[47] Multiple scattering increases the interaction between light and the system and, when gain is added to this scenario, eventually the system lases when stimulated emission dominates over the spontaneous emission of light. No mirrors are needed in a random laser to reach laser action and light scattering, which is generally regarded as a parameter to minimize in standard lasers, and, in fact is the *conditio sine qua non* to observe this effect. Standard random lasers output properties are fixed *a priori* by the gain medium and the emission wavelength is determined by the maximum of the gain curve.

Active photonic glasses have been proposed as a route to exert control over the lasing parameters through the material nanostructure itself and to control the laser output.[48,49] Due to the monodispersity of its scatterers, resonant behavior in

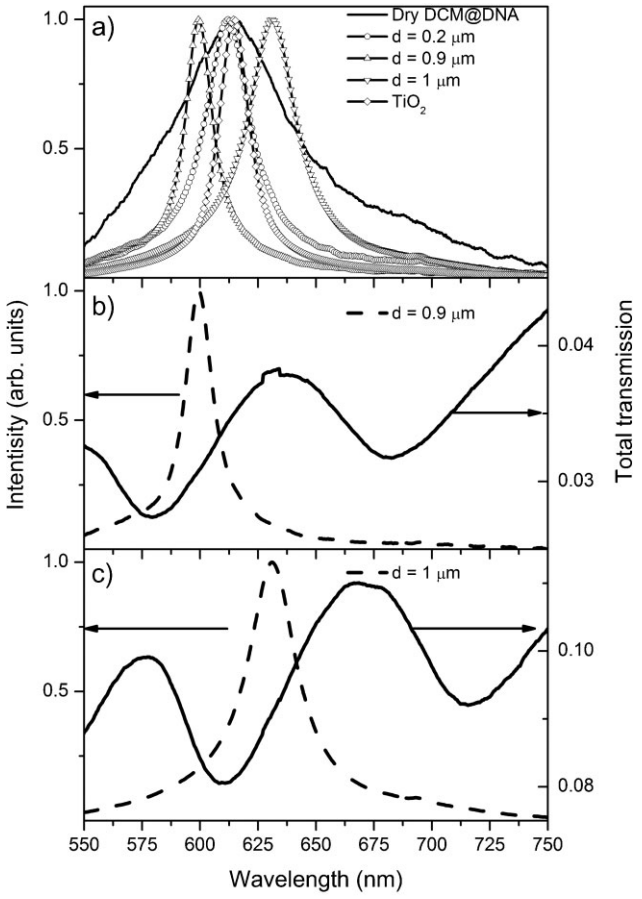

Figure 7. a) Random laser emission from photonic glasses with different sphere diameter compared with the pure dry dye fluorescence and a reference sample made with TiO_2 powder doped with DCM/DNA. The pump energy for every sample is around 10 mJ. b,c) Emission intensity and total transmission for photonic glasses respectively with $d = 0.9$ and $d = 1.0\,\mu m$. Lasing occurs close to the transmission minimum.

diffuse light though a photonic glass allows control of laser emission via the diameter of the spheres and their refractive index. Such a system is a dispersive random device with an *a priori* designed lasing peak within the gain curve. In a photonic glass, therefore, the lasing wavelength becomes very sensitive to the diameter of the constituent spheres and follows the resonances of the system. Figure 7 shows how the modes sustained by the spheres affect the laser output. As a reference we consider a photonic glass of very small spheres with $d = 0.2\,\mu m$ (Fig. 7a, dotted/light blue curve) as well as a polydisperse TiO_2-based random laser (solid/violet curve). Both systems, for different reasons, do not show resonances in static or dynamic measurements.[46,50] They both lase at nearly the same wavelength and close to the maximum of the gain curve. In the same figure, instead, one can observe a controlled overall shift of the lasing wavelength of about 35 nm between different photonic glasses composed with spheres with diameters $d = 0.9\,\mu m$ (triangles) and $d = 1.0\,\mu m$ (inverted triangles). Lasing modes from both systems are shifted with respect to the gain maximum; this can be explained in terms of Mie modes. Figure 7b and c compare the lasing wavelength dependence with the sample total transmission. For these two photonic glasses, the Mie resonances are pronounced, with maxima and minima shifted, even if the difference in the diameter is only $\sim 0.1\,\mu m$. A minimum in transmission corresponds with a maximum in the scattering strength of the system. Light with this wavelength populates a Mie mode in the structure and dwells longer in the spheres, enhancing the light/dye interaction. Thus, the system tends to lase where the scattering strength is maximum, even far from the gain maximum. The limited gain puts a limit on the wavelength shift induced by the scattering resonance.

6. Conclusions

The realization of photonic glasses – solid random distributions of monodisperse spheres – has been demonstrated to be a new encouraging route by which light diffusion can be controlled. The novel material for photonics is a self-assembled *designed disordered* material where the building blocks are identical dielectric spheres. By manipulating the colloidal suspensions, we can switch on or off the ordering process, giving rise to a self-assembly process that provides very thick and completely random solid samples. These materials combine light dispersion with light diffusion, a mix that is crucial to control the diffuse flow of light analogous to how photonic crystals behave for ballistic light. Photonic glasses exhibit resonances in the diffuse light transport parameters: resonant transport mean free path, diffusion constant, and energy velocity. Active photonic glasses can be used to control random lasing and design the lasing emission wavelength. The high contrast of the dielectric in air secures strong light-matter interaction; the Mie resonances provide spectral selectivity, opening a novel route to active disorder-based photonic devices. Photonic glasses are expected to be important for the field of Anderson localization of light, which could be achieved for some resonant wavelength ranges if the refractive index of the material were increased as, for example, in silicon photonic glasses.[51] Photonic glasses by themselves or integrated with photonic crystals may give rise to new applications in future photonic devices.

Acknowledgements

This work was partially funded by the Spanish Ministry of Science and Innovation under contract MAT2006-09062 and Nanolight.es (CSD2007-0046). The authors acknowledge Dr. M. Ibisate and Dr. A. Altube for fruitful discussions.

Received: March 8, 2009
Published online: August 3, 2009

[1] E. Yablonovitch, *Phys. Rev. Lett.* **1987**, *58*, 2059.
[2] S. John, *Phys. Rev. Lett.* **1987**, *58*, 2486.
[3] C. López, *Adv. Mater.* **2003**, *15*, 1679.
[4] P. Sheng, *Introduction to Wave Scattering, Localization, and Mesoscopic Phenomena*, Academic Press, San Diego **1995**.

[5] a) H. Takayasu, *Fractals in Physical Science*, Manchester University, Manchester **1990**. b) M. V. Berry, *J. Phys. A: Math. Gen.* **1979**, *12*, 781. c) J. Uozumi, T. Asakura, in *Current Trends in Optics*, (Ed.: J. C. Dainty), Academic Press, London **1994**, p. 83.
[6] P. V Braun, S. A. Pruzinsky, F. Garcia-Santamaria, *Adv. Mater* **2006**, *18*, 2665.
[7] A. Arsenault, F. Fleischhaker, G. von Freymann, V. Kitaev, H. Miguez, A. Mihi, N. Tetreault, E. Vekris, I. Manners, S. Aitchison, D. Perovic, G. A. Ozin, *Adv. Mater.* **2006**, *18*, 2779.
[8] A. Ledermann, L. Cademartiri, M. Hermatschweiler, C. Toninelli, G. A. Ozin, D. S. Wiersma, M. Wegener, G. von Freymann, *Nat. Mater.* **2006**, *5*, 942.
[9] a) D. Langevin, M. A. Bouchiat, *J. Phys. (Paris) C* **1975**, *1*, 197. b) A. Yu, Val'kov, V. P. Romanov, *Zh. Eksp. Teor. Fiz.* **1982**, *83*, 1777. [*Sov. Phys. JET P* **1982**, *56*, 1028].
[10] S. Gottardo, S. Cavalieri, O. Yaroshchuk, D. S. Wiersma, *Phys. Rev. Lett.* **2004**, *93*, 263901.
[11] P. M. Johnson, B. P. J. Bret, J. G. Rivas, J. J. Kelly, A. Lagendijk, *Phys. Rev. Lett.* **2002**, *89*, 243901.
[12] P. Barthelemy, J. Bertolotti, D. S. Wiersma, *Nature* **2008**, *453*, 495.
[13] M. P. van Albada, A. Lagendijk, *Phys. Rev. Lett.* **1985**, *55*, 2692.
[14] P. E. Wolf, G. Maret, *Phys. Rev. Lett.* **1985**, *55*, 2696.
[15] M. A. Noginov, *Solid-State Random Lasers*, Springer, Berlin **2005**.
[16] a) P. W. Anderson, *Phys. Rev.* **1958**, *109*, 1492. b) P. W. Anderson, *Philos. Mag. B* **1985**, *52*, 505.
[17] A. Z. Genack, N. Garcia, W. Polkosnik, *Phys. Rev. Lett.* **1990**, *65*, 2129.
[18] N. Garcia, A. Z. Genack, *Phys. Rev. Lett.* **1989**, *63*, 259.
[19] H. Cao, Y. G. Zhao, H. C. Ong, S. T. Ho, J. Y. Dai, J. Y. Wu, R. P. H. Chang, *Appl. Phys. Lett.* **1998**, *73*, 3656.
[20] D. S. Wiersma, P. Bartolini, A. Lagendijk, R. Righini, *Nature* **1997**, *390*, 671.
[21] J. Gomez Rivas, R. Sprik, L. D. Noordam, C. W. Rella, A. Lagendijk, *Phys. Rev. E* **2000**, *62*, R4540.
[22] N. Garcia, A. Z. Genack, *Phys. Rev. Lett.* **1991**, *66*, 1850.
[23] X. H. Wu, A. Yamilov, H. Noh, H. Cao, E. W. Seelig, R. P. H. Chang, *J. Opt. Soc. Am. B* **2004**, *21*, 159.
[24] R. H. J. Kop, P. de Vries, R. Sprik, A. Lagendijk, *Phys. Rev. Lett.* **1997**, *79*, 4369.
[25] M. Reufer, L. F. Rojas-Ochoa, S. Eiden, J. J. Saenz, F. Scheffold, *Appl. Phys. Rev.* **2007**, *91*, 171904.
[26] N. M. Lawandy, R. M. Balachandran, A. S. L. Gomes, E. Sauvain, *Nature* **1994**, *368*, 436.
[27] L. F. Rojas-Ochoa, J. M. Mendez-Alcaraz, J. J. Saenz, P. Schurtenberger, F. Scheffold, *Phys. Rev. Lett.* **2004**, *93*, 073903.
[28] Y. Xia, B. Gates, Y. Yin, Y. Lu, *Adv. Mater.* **2000**, *12*, 693.
[29] P. Jiang, J. F. Bertone, K. S. Hwang, V. L. Colvin, *Chem. Mater.* **1999**, *11*, 2131.
[30] J. Ballato, J. Dimaio, A. James, E. Gulliver, *Appl. Phys. Lett.* **1999**, *75*, 1497.
[31] B. V. Derjaguin, L. Landau, *URSS* **1941**, *14*, 633.
[32] E. J. W. Verwey, J. T. G. Overbeek, *Theory of the Stability of Lyophobic Colloids*, Elsevier, Amsterdam **1948**.
[33] K. L. Wu, S. K. Lai, *Langmuir* **2005**, *21*, 3238.
[34] J. W. Goodwin, J. Hearn, C. C. Ho, R. H. Ottewill, *Colloid Polym. Sci.* **1974**, *252*, 464.
[35] M. Mueller, R. Zentel, T. Maka, S. G. Romanov, C. M. Sotomayor Torres, *Chem. Mater.* **2000**, *12*, 508.
[36] J. L. Baldwin, B. A. Dempsey, *Colloids Surf, A* **2001**, *177*, 111.
[37] D. A. Weitz, *Science* **2004**, *303*, 968.
[38] P. Lodahl, A. F. van Driel, I. S. Nikolaev, A. Irman, K. Overgaag, D. Vanmaekelbergh, W. L. Vos, *Nature* **2004**, *430*, 654.
[39] V. M. Markushev, V. F. Zolin, C. M. Briskina, *Zh. Prikl. Spektrosk.* **1986**, *45*, 847.
[40] R. M. Balachandran, N. M. Lawandy, J. A. Moon, *Opt. Lett.* **1997**, *22*, 319.
[41] M. Bahoura, K. J. Morris, M. A. Noginov, *Opt. Commun.* **2002**, *201*, 405.
[42] S. Klein, O. Cregut, D. Gindre, A. Boeglin, K. D. Dorkenoo, *Opt. Express* **2005**, *3*, 5387.
[43] R. C. Polson, Z. V. Vardeny, *Appl. Phys. Lett.* **2004**, *85*, 1289.
[44] a) J. P. Jacopsen, J. B. Pedersen, D. E. Wemmer, *Nucl. Acid Res.* **1995**, *23*, 753. b) P. D. Garcia, M. Ibisate, R. Sapienza, C. Lopez, *Phys. Rev. A*, **2009**, in press.
[45] G. Mie, *Ann. Phys.* **1908**, *25*, 77.
[46] R. Sapienza, P. D. Garcia, J. Bertolotti, M. D. Martin, A. Blanco, L. Viña, C. López, D. S. Wiersma, *Phys. Rev. Lett.* **2007**, *99*, 233902.
[47] D. S. Wiersma, *Nat. Phys.* **2008**, *4*, 359.
[48] S. Gottardo, Riccardo. Sapienza, P. D. Garcia, A. Blanco, D. S. Wiersma, C. Lopez, *Nat. Photonics* **2008**, *2*, 429.
[49] P. D. Garcia, M. Ibisate, R. Sapienza, D. S. Wiersma, C. Lopez, *Phys. Rev. A.* **2009**, submitted.
[50] P. D. Garcia, R. Sapienza, J. Bertolotti, M. D. Martin, A. Blanco, A. Altube, L. Viña, D. S. Wiersma, C. López, *Phys. Rev. A* **2008**, *78*, 023823.
[51] M. Ibisate, D. Golmayo, C. López, *Adv. Mater.* **2009**, DOI:10.1002/adma.200900188.